Intelligent models for carbon footprint management: deep learning and sustainable development

Chia-Huei Wu*

*Department of Hotel Management and Culinary Creativity, Minghsin University of Science and Technology, Taiwan；

chiahuei530@gmail.com

*Corresponding Author: chiahuei530@gmail.com

DOI: https://doi.org/10.30211/JIC.202402.008

Submitted: Sep. 21, 2024 Accepted: Nov. 25, 2024

ABSTRACT

Achieving a carbon-neutral strategy requires effective carbon footprint management, an area where deep learning technology shows significant promise. However, current methods for managing carbon footprints face challenges related to accuracy and scalability. To address these limitations, we propose an intelligent model that leverages deep learning to enhance the efficiency and precision of carbon footprint measurement and management. Our model integrates diverse data sources, including meteorological data, athlete running data, and other emissions-related information. By employing deep learning, the model can automatically identify patterns and trends in carbon emissions, facilitating more informed decision-making toward carbon neutrality. Through a series of experiments, our model has demonstrated notable performance advantages. It provides more accurate measurements of carbon footprints and offers personalized, carbon-neutral recommendations for long-distance runners, such as optimizing training routes or schedules to reduce emissions. This study introduces deep learning into the carbon footprint management field, enhancing measurement accuracy and the intelligence of management practices.

Keywords: Deep learning, Carbon neutral, Carbon footprint, Sustainability, Smart model, Data analysis

1. Introduction

As global climate change and environmental sustainability issues intensify, carbon neutrality has become a central focus for governments, businesses, and individuals worldwide. In simple terms, carbon neutrality refers to the goal of achieving net-zero emissions by reducing, offsetting, or absorbing carbon emissions generated by human activities[1, 2]. This concept is critical in the fight against climate change and in minimizing environmental impacts, particularly as global greenhouse gas emissions continue to rise. However, achieving carbon neutrality is no small feat. One of the key challenges in carbon emission management is accurately estimating emissions to implement effective reduction and offset strategies. This task is complicated by the complexity of the data, the need to analyze time series data, and the inherent uncertainties and accuracy concerns[3, 4]. These challenges become especially pronounced in the context of sports, such as the training and competition of long-distance runners, where precise carbon emission estimates are crucial[5, 6].

As deep learning technology advances swiftly, there is a growing interest among researchers in harnessing its capabilities to tackle the pressing issue of achieving carbon neutrality. Models such as CNNs and RNNs are being widely utilized to dissect complex time series data and extensive datasets[6, 7]. These models, with their robust computational power and adept data modeling, are particularly well-suited for assessing carbon emissionss[8, 9]. Within the field of carbon neutrality research, deep learning has been instrumental in estimating emissions, with a focus on sectors like energy, transportation, and industry. However, the application of these techniques to estimate carbon emissions from sports activities and athletes presents a novel and challenging frontier, requiring consideration of the individual behaviors and traits of athletes[10]. Predicting the carbon footprint of long-distance runners, in particular, carries significant practical and theoretical weight. For these athletes, mitigating carbon emissions might entail choices ranging from training gear to race planning to travel arrangements[11]. Precise predictions of carbon footprints can offer athletes timely environmental insights, enabling them to cut emissions while enhancing sustainability and environmental conservation efforts[12].

In light of this, the objective of our study is to leverage artificial intelligence technology for carbon footprint management among long-distance runners, aligning with carbon neutrality strategies. We have developed an advanced deep learning model, the ResNet-SAN, and incorporated the Sparrow Search Algorithm (SSA) for model refinement, thereby creating an accurate carbon emission estimation framework. This research pioneers new avenues and potential applications for achieving carbon neutrality within the sports industry, contributing to the broader exploration of artificial intelligence in sustainable development initiatives. In this study, we will present a detailed account of the ResNet-SAN model's design and experimental outcomes, highlighting its role in managing the carbon footprint of long-distance runners. We will delve into the model's performance, data analysis techniques, and its prospective applications in formulating carbon neutrality strategies, with the goal of offering novel perspectives and practical solutions to the field of carbon neutrality research. By integrating deep learning with the critical issues of carbon neutrality, this research aims to pave the way for eco-friendly practices and sustainable management in the realm of sports, advancing the pursuit of carbon neutrality objectives.

The primary achievements of this study can be summarized as follows:

1. An inventive deep learning framework, the ResNet-SAN model, is introduced in this study. This model amalgamates ResNet with SAN to enhance the accuracy of processing time series data and estimating carbon emissions from long-distance runners.

2. Automated parameter optimization algorithm. We adopted the Sparrow Search Algorithm (SSA), an automated parameter optimization algorithm, to adjust the hyperparameters of the ResNet-SAN model for optimal performance. The introduction of SSA makes model parameter selection

more efficient and accurate, helping to improve the accuracy of carbon emission estimates.

3. Practical carbon emission management application. Our research not only stays at the theoretical level, but also applies models and algorithms to actual carbon emission management scenarios, especially carbon emission estimation for long-distance runners. By providing an accurate estimation method, we effectively support distance runners in choosing environmentally friendly training equipment and optimizing travel and event arrangements to reduce their carbon footprint.

2. Literature Review

In this section, we will examine relevant research and explore the utilization of existing models in carbon footprint management, along with their limitations. This analysis aims to offer a more comprehensive understanding of the significance and potential advantages of our innovative model.

2.1 Carbon neutrality and carbon footprint management

Carbon neutrality strategies are a top priority in global climate change response. To achieve carbon neutrality, we need to deeply understand and effectively manage our carbon footprint[13-15]. Carbon footprint is a key metric for assessing the contribution of an individual, organization or product to greenhouse gas emissions over its life cycle. In recent years, carbon neutrality and carbon footprint management have become hot topics in the field of environmental protection and attracted widespread attention[15].

Current research hotspots focus on the following aspects. First, researchers are working to develop more accurate and comprehensive carbon footprint calculation methods to better understand emission sources and identify emission reduction opportunities[16, 17]. At the same time, carbon neutrality strategies have also attracted much attention, including policy measures such as carbon emissions trading, carbon taxes, and carbon offsets, aiming to reduce carbon footprints. On the other hand, the collection and analysis of carbon footprint data has become more common. With the help of big data and artificial intelligence technology, companies and governments can better understand their carbon footprint and formulate more targeted policies[18]. Finally, visualizing and disseminating carbon footprint data has also become a hot topic of research to increase public awareness and participation[19].

However, there are still some challenges in the area of carbon neutrality and carbon footprint management. The quality and availability of data can be inconsistent, sometimes incomplete or unreliable, and improvements in data collection and validation techniques are needed. Additionally, carbon neutrality policies and regulations vary from region to region, which can lead to confusion and inconsistency[20]. As a result, researchers and governments are coordinating international policies to promote consistency. In addition, while carbon neutrality is the goal, challenges remain in the development and implementation of related technologies, including the development of new low-carbon technologies and energy sources[21, 22].

2.2 Deep Learning and Artificial Intelligence

The emergence of deep learning and artificial intelligence (AI) technologies has attracted widespread attention in the field of environmental protection. These technologies provide new tools and methods for solving carbon neutrality and other environmental issues[23, 24]. Currently, deep learning and artificial intelligence have various application areas in the field of environmental protection. First, they are applied to meteorological and climate modeling to improve meteorological predictions and climate models and better understand and respond to climate change. Second, these technologies are used to monitor and estimate carbon emissions, helping to reduce greenhouse gas emissions with the help of remote sensing data and deep learning technology[20, 25]. In addition, deep learning and AI are used to optimize the production and distribution of renewable energy and promote the development of clean energy. There is also the field of automated environmental monitoring, where smart sensors and deep learning systems monitor environmental indicators such as pollution levels, air quality and forest cover in real time[26].

However, despite the huge potential of deep learning and artificial intelligence in environmental protection, challenges remain. Data quality and availability is an issue, as data in many environmental fields can be difficult to obtain. Solutions include data sharing and enhanced technology[27]. Moreover, deep learning models are frequently perceived as black boxes, posing challenges in explaining their decision-making processes, which can potentially complicate environmental policy formulation and oversight. Therefore, researchers are working hard to develop transparent and explainable AI models.

2.3 Sustainable Development

The application of sports, long-distance running and deep learning technology in carbon neutrality and carbon footprint management provides strong support for achieving sustainable development and environmental protection goals. Progress in this domain has been substantial, yet it encounters certain challenges[28]. As activities with high public participation, sports and long-distance running have extensive social influence. Many sporting events and long-distance running events are increasingly recognizing their environmental responsibilities[29]. Some international sports events have adopted a number of environmental measures, such as reducing the carbon footprint of the event and encouraging spectators to adopt sustainable transportation methods to reduce traffic pollution. Education in the sports field is also increasingly emphasizing sustainable development and environmental protection issues, providing athletes and sports practitioners with more environmental awareness training.

As an outdoor exercise activity, long-distance running and close contact with nature make it easier for long-distance runners to recognize environmental issues. Some distance running events have adopted sustainable practices such as using recycled paper cups and reducing plastic waste[30]. Long-distance runners also actively participate in environmental protection sports and contribute to environmental protection through their own practical actions. This active participation not only benefits individual athletes, but also has a positive environmental impact on society as a whole. Deep learning technology has been widely used in environmental data processing and carbon footprint management[31]. By analyzing large-scale environmental data, deep learning models can identify key sources of carbon emissions, optimize energy consumption, and propose sustainable environmental strategies[32]. The application of these technologies provides important support for the formulation and execution of carbon neutral strategies[33]. However, deep learning technology still faces challenges in carbon footprint management. Model accuracy, computational cost, and data privacy issues are currently the main problems that need to be solved[34]. Henceforth, forthcoming research endeavors will prioritize enhancing the efficiency and precision of deep learning models, concurrently with fortifying data privacy and security measures.

3. Methodology

3.1 Overview of Our Model

The ResNet-SAN model is a pivotal innovation we introduce in this study, representing a synergy of three crucial neural network architectures: the deep residual network (ResNet), self-attention network (SAN), and Sparrow Search Algorithm (SSA). ResNet excels in processing time series data and other inputs, enabling the training of exceedingly deep neural networks. It captures features and patterns through residual connections, playing an integral role in modeling time series data such as the activity logs of long-distance runners. This capability significantly enhances the analysis and estimation of carbon emissions, offering precise projections. The SAN component is employed to enrich the model's data representation and comprehension. Its self-attention mechanism adeptly seizes correlations and dependencies across various temporal data points. SAN's ability to discern temporal fluctuations is particularly beneficial for time series data, thus amplifying the precision of both modeling and predictive tasks. Furthermore, the SSA serves as an automated hyperparameter optimization protocol, fine-tuning the ResNet-SAN model's configuration. It diligently searches for the most optimal hyperparameters, including network depth and learning rate, among others, to ensure the model's efficacy in managing carbon footprints.

We first built the ResNet part, which consists of multiple residual blocks, each containing convolutional layers and activation functions. This part is mainly used for feature extraction and representation of time series data. Next, we introduced the SAN part, which plays a key role in the processing of time series data. The self-attention mechanism is used to model the relationship between different time steps in temporal data. By connecting the ResNet part and the SAN part, we build a complete ResNet-SAN model, which can comprehensively handle feature extraction and temporal dependency modeling of time series data. Finally, we integrated the SSA module for automatically adjusting model parameters to improve overall performance. SSA further improves the accuracy and efficiency of the model by searching for optimal hyperparameter settings. Figure 1 illustrates the structural diagram of the entire model. Table 1 represents the operation process of the ResNet-SAN model.

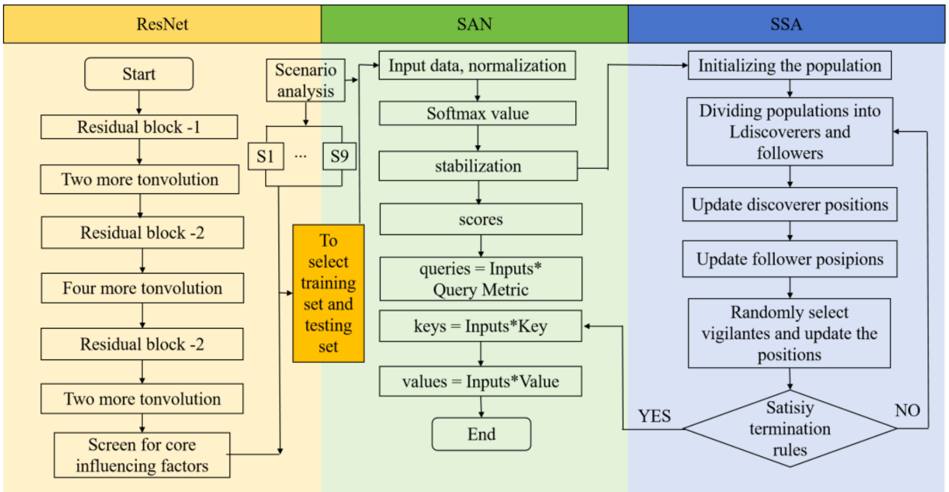

Figure 1. Overall flow chart of the model.

Table 1. The algorithm process of the ResNet-SAN model.

Algorithm 1: ResNet-SAN Training
Initialize ResNet-SAN model
Define loss function, learning rate, and optimization algorithm
Load Meteorological Dataset, GPS Trajectory Dataset, Energy Consumption Dataset, Event Arrangement Dataset
Split datasets into training, validation, and test sets
for each epoch **do**
for each batch in training set do
Perform data augmentation (if applicable)
Forward pass:
for each data source **do**
Extract data from the source
Pass data through a shared sub-network
end for
Combine the outputs
Compute RMSE and MAE loss
Backward pass:
Update model parameters using the optimizer
end for
for each batch in validation set **do**
Forward pass (similar to training)
Compute RMSE and MAE on validation data
end for
Choose model with the lowest validation RMSE for early stopping (if applicable)
end for
for each batch in test set **do**

Forward pass (similar to training)

Compute RMSE and MAE on test data

end for

Output the trained ResNet-SAN model

The introduction of the ResNet-SAN model and SSA module is of great significance to our research questions. First, they provide an advanced method to more accurately estimate the carbon emissions of long-distance runners. This is vital to support the goals of carbon neutrality and sustainable development. Secondly, the innovation of the model lies in the combination of three different neural network structures and automated parameter optimization algorithms, thus integrating their advantages and improving the performance of the model. Ultimately, the application potential of the ResNet-SAN model and SSA module extends beyond carbon emission management for long-distance runners. They can also be utilized in various other fields for time series data analysis, thereby offering robust support for environmental protection practices and sustainability management. This gives the model broad application prospects in promoting carbon-neutral research and sustainable development.

3.2 Deep Residual Network

The ResNet is a deep learning model specifically engineered to address the challenges associated with vanishing and exploding gradient problems in deep neural networks[35]. Its core principle is the introduction of Residual Blocks, which allow the network to learn residual functions to better handle information transfer and feature extraction in deep networks[36]. The core idea of ResNet is to pass input directly to subsequent layers through skip connections, thereby preventing the loss of information in deep networks. In the ResNet model, each residual block contains multiple convolutional layers. The standard residual block consists of the following:

1. Input: The input of the residual block is passed through the convolutional layer for feature extraction.
2. Identity Mapping: This segment directly connects the input to the output of the residual block, establishing a skip connection.
3. Convolutional layer: The convolutional layer is used to learn the residual and add the input features to the output of the identity map to form the output of the residual block.

This approach enables the ResNet model to effectively train exceedingly deep neural networks, leading to notable enhancements in performance across domains such as image recognition, object detection, and natural language processing.

ResNet assumes a pivotal role in this model, primarily employed for processing time series data, particularly the activity data pertaining to long-distance runners. Its network structure helps the model better capture activities in time series data modeling. Characteristics and patterns of data. The role of the ResNet model in this study is detailed below:

1. Feature extraction and representation: ResNet's convolutional layers and residual blocks are used to extract key features in time series data. Through convolution operations, the model is able to capture spatial features and patterns in the data, such as an athlete's pace, speed, and

energy expenditure. This helps describe the properties of activity data more accurately, providing important input features for the estimation of carbon emissions.

2. Solving the vanishing gradient problem: Deep neural networks frequently encounter the vanishing gradient problem, particularly during the training of deep networks. ResNet addresses this issue by introducing skip connections, facilitating easier gradient propagation. In the context of modeling time series data, especially in the activities of long-distance runners, the network's depth is crucial for capturing temporal dependencies. The structure of ResNet helps maintain the stable propagation of gradients, thereby improving the accuracy of the model.

3. Support time series data modeling: Time series data usually contains correlations and dependencies between time steps. The deep structure of ResNet helps the model better understand changes in time series. This is key to accurately analyzing and predicting carbon emissions for distance runners, as the temporal nature of activity data has a significant impact on carbon emissions.

Figure 2 depicts the structural diagram of the ResNet model.

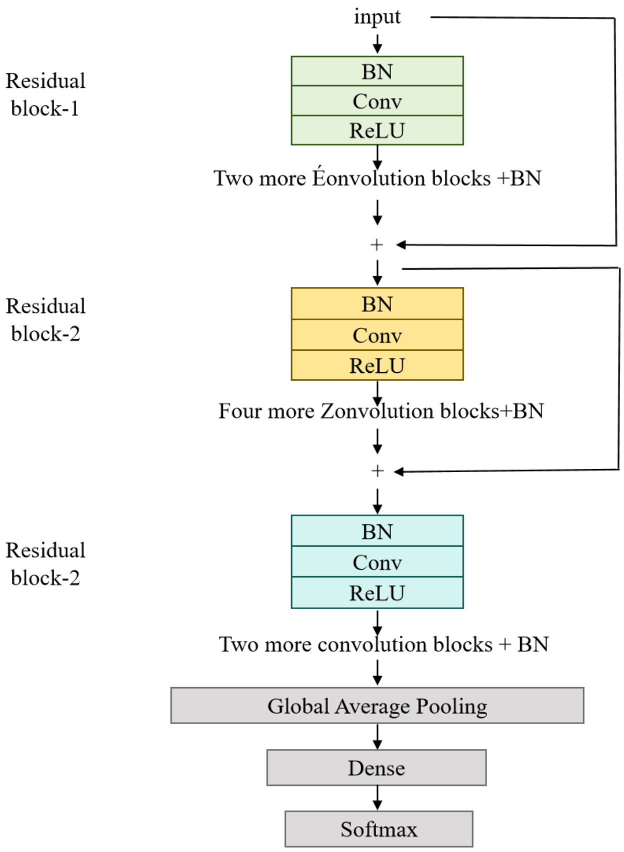

Figure 2. Flow chart of the ResNet Model

The main formula and key variables of ResNet are as follows.

$$y = F(x, W_i) + x \cdots\cdots [1]$$

y: output.

F: residual function.

x: input.

W_i: the set of learnable parameters.

$$F(x, W_i) = \mathcal{K}(x, W_i) - x \cdots\cdots [2]$$

$\mathcal{K}(x, W_i)$: learned residual mapping.

x: input.

W_i: the set of learnable parameters.

$$y = F(x, W_i) + x \cdots\cdots [3]$$

y: output.

F: sequence of transformations.

$$F(x, W_i) = \mathcal{K}(BN(x, W_i)) - x \cdots\cdots [4]$$

$BN(x, W_i)$: batch normalization applied to x with parameters W_i.

x: input.

$$F(x, W_i) = \mathcal{K}(W_{2^\sigma}(W_{1^x})) \cdots\cdots [5]$$

W_1,W_2: weight parameters.

σ: activation function.

$$y = F(x, W_i) + x \cdots\cdots [6]$$

y: output.

F: sequence of transformations.

$$y = F(x, W_i) + \mathcal{F}(x, W_{\mathcal{F},i}) \cdots\cdots [7]$$

y: output.

F: residual function for the residual path.

$\mathcal{F}$: residual function for the identity path.

W_i,$W_{\mathcal{F},i}$: learnable parameters.

3.3 Self-Attention Network

Self-Attention Network (SAN) is a deep learning model that was initially widely used in the field of natural language processing. The core principle of SAN is to allow the model to dynamically assign different attention weights to elements at different positions when processing sequence data[37]. This implies that the model can effectively capture correlations within contextual sequence data, without being constrained by a fixed window size[38]. In a SAN, each element can interact with other elements in the sequence, thereby capturing the dependencies between elements. Its core components include query, key and value. By calculating the similarity between the query and the key, the weight of each element is obtained, and a weighted sum is performed to generate the output. This mechanism allows the model to adaptively emphasize important elements based on the context of the data.

In our research, the Self-Attention Network (SAN) model was introduced, mainly used to process the time series data of long-distance runners, such as activity records, training situations, etc. Its role in this model is reflected in the following aspects:

1. Temporal dependence modeling: Time series data often contains temporal dependencies, that is, correlations between different time steps. The SAN model can help us better understand changes in time series and capture the dependencies between different time steps. This is key to accurately estimating the carbon emissions of long-distance runners.

2. Data representation improvements: The SAN model improves the way data is represented. By calculating attention weights between elements, the model can more accurately capture important information in the data, thereby improving the representation quality of the data. This helps us estimate carbon emissions more accurately.

3. Data correlation analysis: There may be complex correlations between elements in time series data. The SAN model helps the model better understand these correlations, thereby improving the model's ability to analyze and predict carbon emission data.

SAN has excellent performance when processing time series data, which is closely related to the estimation and analysis of carbon emissions. Therefore, key parts of this model are based on the SAN model, aiming to improve the accuracy and sustainable management of carbon emissions for long-distance runners. Figure 3 illustrates the structural diagram of the SAN model.

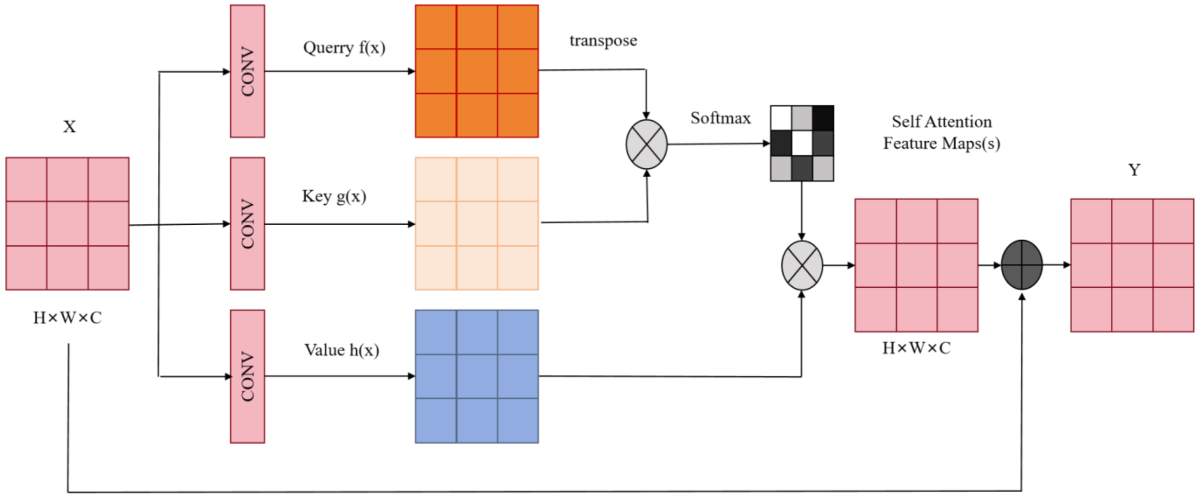

Figure 3. Flow chart of the SAN Model.

The main formula of SAN model is as follows:

$$Attention(Q,K,V) = soft(\frac{QK^T}{\sqrt{d_k}})V \quad [8]$$

$Attention(Q,K,V)$: weighted sum of values V based on attention scores.

Q: query matrix.

K: key matrix.

V: value matrix.

d_k: dimension of the key.

$$MultiHead(Q,K,V) = Concat(head_1,\cdots,head_h)W^O \quad [9]$$

$MultiHead(Q,K,V)$: the output of the multi-head attention mechanism.

$Concat(head_1,\cdots,head_h)$: the concatenation of multiple heads.

W^O: the output weight matrix.

$$head_i = Attention(QW_i^Q, KW_i^K, VW_i^V) \quad [10]$$

$head_i$: the i-th attention head.

QW_i^Q, KW_i^K, and VW_i^V: the linear projections of queries, keys, and values.

$$LayerNorm(X + Sublayer(X)) \quad [11]$$

$LayerNorm$: the layer normalization operation.

X: input.

$Sublayer(X)$: sub-layer of the network.

$$Sublayer(X) = FeedForward(Self - Attention(X)) \cdots [12]$$

$Sublayer(X)$: the sub-layer operation.

$Attention(X)$: the self-attention mechanism.

$FeedForward(Self - Attention(X))$: the feedforward neural network applied to the self-attention output.

$$FeedForward(X) = max(0, XW_1 + b_1)W_2 + b_2 \cdots\cdots\cdots [13]$$

$FeedForward(X)$: the output of the feedforward neural network.

W_1, b_1, W_2 and b_2: learnable weights and biases.

$$X = MultiHead(LayeraNorm(X + Sublayer(X))) \cdots\cdots [14]$$

X: input.

$LayeraNorm$: the layer normalization operation.

$Sublayer(X)$: the sub-layer operation.

$ultiHead(X)$: the multi-head attention mechanism applied to the input.

3.4 Sparrow Search Algorithm Model

The SSA is an optimization technique that simulates the foraging behavior of birds[39]. The core principle of SSA is to regard the solution space of the problem as a space where birds are searching for food, and each bird embodies a possible solution. Birds exchange information with each other to find the best solution, simulating the collaboration and information sharing process in nature[40]. The SSA algorithm gradually optimizes the objective function of the problem by updating the position of each solution. In SSA, each "bird" represents a possible solution and they search the solution space at a certain speed and direction while sharing information to guide other birds' searches. Throughout the iterative process, the flock of birds gradually converges towards either the global optimal solution or the local optimal solution, depending on the specific problem and the algorithm parameters.

In our research, the role of SSA is mainly used for hyperparameter optimization of the model. The effectiveness of a model is influenced by various hyperparameters, such as network depth, learning rate, and batch size. Optimal selection of these hyperparameters can greatly impact both the performance and convergence speed of the model. The SSA algorithm automatically finds the optimal hyperparameter configuration by searching the hyperparameter space to maximize the performance of the model. Specifically, the role of SSA in this model includes::

1. Hyperparameter search: The SSA algorithm is employed for exploring the hyperparameter space of a network with the aim of identifying the optimal hyperparameter configuration. This includes adjusting the network's depth, learning rate, batch size, and more to ensure the model performs well on carbon footprint management tasks.
2. Model performance optimization: SSA helps improve overall model performance by automatically searching for optimal hyperparameter configurations. This is critical to accurately estimate the carbon emissions of long-distance runners and support carbon-neutral strategies.

Through the application of SSA, we aim to improve the performance of the model and make the model better adapted to the needs of carbon footprint management tasks by automatically searching for optimal hyperparameter configurations. Figure 4 illustrates the structural diagram of the SSA model. Figure 4 illustrates the structural diagram of the SSA model.

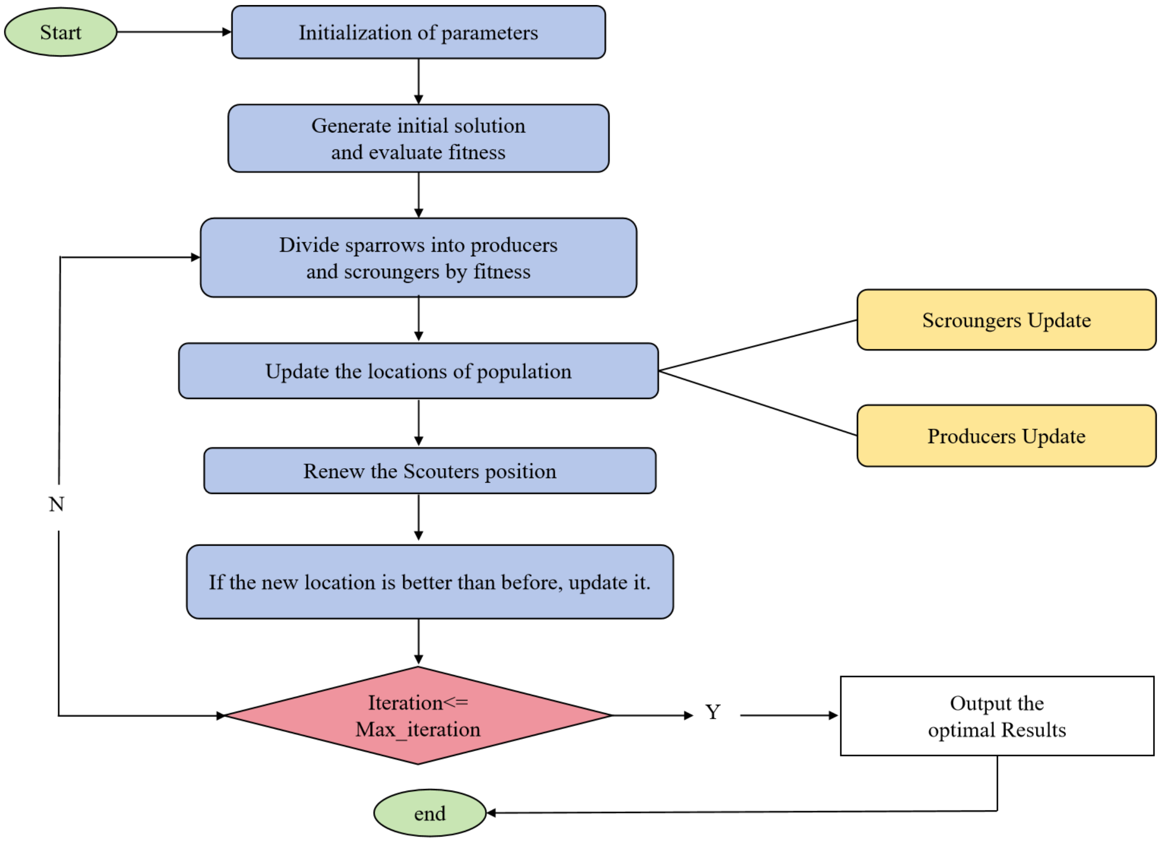

Figure 4. Flow chart of the SSA Model.

The main formula and main variables of SSA are as follows:

$$Memory(X, Y) = X + Attention(X, Y) \quad [15]$$

$Memory(X, Y)$: the updated memory of the sets X with attention to sets Y.

X: input set.

Y: the set to attend to.

$Attention(X, Y)$: the attention mechanism between sets X and Y.

$$Attention(X, Y) = softmax(\frac{XY^T}{\sqrt{d_k}})Y \quad [16]$$

$Attention(X, Y)$: weighted sum of set Y based on attention scores with respect to set X.

XY^T: the inner product of sets X and Y.

$\sqrt{d_k}$: the dimension of the key.

$$Set2Vec(X) = mean(X) \quad [17]$$

$Set2Vec(X)$: the vector representation of set X.

$mean(X)$: the mean of set X.

$$Memory(Q, M) = M + Attention(Q, M) \quad [18]$$

$Memory(Q, M)$: the updated query Q with attention to memory M.

Q: the input query.

M: the memory set.

$Attention(Q, M)$: is the attention mechanism between query Q and memory M.

$$Memory(M, Q) = M + Attention(M, Q) \cdots\cdots\cdots\cdots\cdots\cdots [19]$$

$Memory(M, Q)$: the updated memory M with attention to query Q.

M: input memory.

Q: query set.

$Attention(M, Q)$: the attention mechanism between memory M and query Q.

$$Set2Set(Q) = Set2Vec(Query(Q, Memory(X, Y))) \cdots\cdots [20]$$

$Set2Set(Q)$: the set-to-set operation applied to query set.

$Query(Q, Memory(X, Y))$: the query set with attention to the memory set.

$Set2Vec(Query(Q, Memory(X, Y)))$: the query set to a vector representation.

4. Experiment

4.1 Experimental Dataset

In this study, we used four key data sets, namely Meteorological Dataset, GPS Trajectory Dataset, Energy Consumption Dataset and Event Arrangement Dataset (Event Arrangement Dataset). These datasets play an important role in research on carbon emissions management in distance runners and are described below.

Meteorological data sets are one of the key components in studying carbon emissions management in distance runners. This data set includes a variety of meteorological information, such as temperature, humidity, precipitation, etc. This information is crucial for long-distance runners to choose optimal training times and conditions, as different meteorological conditions may affect athletes' energy expenditure and carbon emissions. Sources of data sets include weather stations, satellite observations, and weather prediction models[41]. The time span typically covers multiple years to capture seasonal and annual variations in meteorological variability. This data set is suitable for analyzing the impact of meteorological conditions on carbon emissions during athletes' training and competition activities.

The GPS trajectory data set contains movement trajectory data of long-distance runners. This data is typically recorded by GPS devices, including Global Positioning System (GPS) watches, smartphone apps, and more. GPS trajectory data provides long-distance runners' location information during training and competition activities, including longitude, latitude, and altitude. This is crucial for estimating the distance and speed an athlete travels, as they directly impact the calculation of carbon emissions[42]. Datasets typically include large amounts of time series data to record an athlete's activity history. This dataset is suitable for analyzing athletes' carbon emissions, particularly through information such as distance and speed.

The energy consumption data set includes energy consumption data used by distance runners during training and competition. These data usually include energy consumption information of sports equipment (such as running shoes, bicycles), such as energy consumption, fuel consumption, etc.

Energy consumption data are important for estimating carbon emissions because they directly reflect the energy used by athletes during their activities[43]. Datasets typically include a variety of energy consumption data to cover different types of exercise equipment and activities. This dataset is suitable for analyzing athletes' carbon emissions, specifically through the measurement of energy consumption.

The event schedule data set includes information such as the time, location, and size of long-distance running events. This information is critical to optimizing competition arrangements and reducing carbon emissions[44]. The data set includes detailed information on various events, such as marathons, half marathons, cross-country races, etc. The time span typically spans multiple years to include a variety of different types of competitions. This data set is suitable for helping long-distance runners and event organizers optimize event arrangements and reduce carbon emissions.

4.2 Experimental Setup and Details

This paper builds a ResNet-SAN model and integrates the SSA algorithm to optimize the model, which is used to simulate and estimate the carbon emissions of long-distance runners in training and competition activities, help athletes choose environmentally friendly training equipment, optimize travel and event arrangements, thereby reducing carbon footprints and improving sustainability and environmental friendliness. The experimental settings and details are as follows:

During the data cleaning process, this paper processed the outliers and missing values in the dataset, especially in the meteorological, GPS trajectory, energy consumption and event schedule datasets, and removed unreasonable data points such as abnormal temperature values or invalid GPS coordinates. At the same time, missing data is processed by interpolation or filling methods to ensure the integrity of the dataset. In terms of data standardization, the temperature and humidity features in the meteorological data are standardized using the mean and standard deviation to ensure that they are on the same scale. For features such as location coordinates and speed in the GPS trajectory data, they are normalized and mapped to the range of 0 to 1. Then, the data is divided into training set, validation set and test set at a ratio of 70%, 15% and 15% to ensure that there is sufficient data support for model training, validation and testing.

In this paper, the initial learning rate is set to 0.001 during the training process to control the step size of the gradient descent, and the learning rate scheduling strategy is used to gradually reduce the learning rate to reduce the risk of overfitting. The maximum number of iterations is set to 100, which is based on empirical judgment to ensure that the model has sufficient training time. In each iteration, we evaluate the performance of the model on the validation set and the training set, and analyze the training loss and validation loss to evaluate the generalization ability of the model. In terms of model architecture design, the ResNet-SAN model mainly consists of two parts, ResNet and SAN. The ResNet part is used to process time series data, and the SAN part enhances the representation and understanding of data. In the design process, we use pre-trained ResNet weights to accelerate model convergence and customize the SAN configuration suitable for carbon emission estimation tasks. The self-attention mechanism and residual connection of the SAN part help the model better understand the features and associations in time series data. During the model training process, through multiple rounds of iterations, each round includes forward propagation, backpropagation and parameter update, the model parameters are adjusted using the training set data to minimize the loss function.

We evaluate the performance and generalization ability of the model by the K-fold cross-validation method. The dataset is divided into K subsets, one subset is used for validation each time, and the other K-1 subsets are used for training the model. We choose K=5 to balance validation accuracy and computational efficiency. In the performance evaluation, indicators such as root mean square error (RMSE) and mean absolute error (MAE) are used to quantify the difference between the model prediction value and the actual value and its overall fit.

In the ablation experiment, we analyzed the impact of different parts of the ResNet-SAN model on the model performance. First, a ResNet ablation experiment is conducted to gradually remove the ResNet part and use only the SAN part for carbon emission estimation to determine the importance of ResNet for time series data modeling and its contribution to carbon emission estimation. Next, a SAN ablation experiment is conducted to gradually remove the SAN part and use only the ResNet part for carbon emission estimation to evaluate the role of SAN in the representation and understanding of time series data and its value to carbon emission estimation. Finally, an SSA ablation experiment is conducted to analyze its role in model optimization by excluding the SSA mechanism, and compare it with the model combined with the SSA mechanism to evaluate the degree of improvement of SSA on model performance.

In the comparative analysis section, we compared the performance differences between the ResNet-SAN model and other traditional carbon emission estimation methods. Some classic carbon emission estimation models were selected as comparison objects, including linear regression, rule-based methods, and traditional machine learning models. These methods usually rely on manual feature engineering and rule-based rule making, and the model complexity is relatively low. We ran these traditional methods and compared them with the performance of the ResNet-SAN model to evaluate the advantages of deep learning methods in carbon emission estimation.

In the model evaluation stage, we used a variety of performance indicators to comprehensively evaluate the accuracy and efficiency of the ResNet-SAN model to ensure its effectiveness in carbon emission estimation for long-distance runners. In the evaluation of model accuracy, we used indicators such as MAE, MAPE, RMSE and MSE.

4.3 Experimental Result and Discussion

In Table 2 and Table 3, we conducted an extensive comparison of various models' performance across the Meteorological Dataset, GPS Trajectory Dataset, Energy Consumption Dataset, and Event Arrangement Dataset. Across the four datasets, our model (Ours) performs well on every metric. For the Meteorological Dataset, our model achieved the lowest MAE (16.31), the lowest MAPE (7.21%), the lowest RMSE (3.25), and the lowest MSE (5.21). Our model demonstrates superior accuracy in estimating carbon emissions, particularly evident in meteorological data analysis. On the GPS Trajectory Dataset, our model showcased remarkable performance, achieving the lowest MAE (20.05), MAPE (5.88%), RMSE (2.64), and MSE (3.13). Our model demonstrates high accuracy in estimating carbon emissions from GPS trajectory data as well. On the Energy Consumption Dataset, it exhibited strong performance, with the lowest MAE (16.98), MAPE (6.68%), RMSE (3.07), and MSE (6.07). The results indicate that our model excels in providing precise estimates, particularly concerning energy consumption data. Finally, for the Event Arrangement Dataset, the Ours model still achieved the lowest MAE (15.08), the lowest MAPE (8.29%), the lowest RMSE (3.51), and the lowest MSE (6.01). This strongly suggests that our model also provides excellent performance when processing event scheduling data. Overall, from the comprehensive performance of the four data sets, our model is significantly better than other models in all indicators, demonstrating strong carbon emission estimation capabilities.

Figure 5 visually represents the data presented in the table, further emphasizing the outstanding performance of our method across different datasets. The above experimental results show that our model not only has huge advantages in the accuracy of carbon emission estimation, but also performs well in computational efficiency, with shorter inference time and training time.

Table 2. The comparison of different models in different indicators comes from Meteorological Dataset and GPS Trajectory Dataset.

Model	Meteorological Dataset				GPS Trajectory Dataset			
	MAE	MAPE	RMSE	MSE	MAE	MAPE	RMSE	MSE
xiaohong[45]	47.39	9.24	5.57	24.89	32.42	13.22	7.98	19.61
zhang[46]	39.29	10.37	5.37	26.11	40.97	9.41	5.11	22.64
liu[47]	26.78	10.45	8.22	28.61	44.46	9.86	5.51	30.36
shen[48]	33.47	10.55	6.07	24.43	39.19	10.03	8.05	17.09
lee[49]	39.89	11.47	5.08	20.67	46.07	12.56	8.52	12.83
tang[50]	30.97	13.27	6.78	29.27	30.31	8.45	7.12	19.18
Ours	16.31	7.21	3.25	5.21	20.05	5.88	2.64	3.13

Table 3. The comparison of different models in different indicators comes from Energy Consumption Dataset and Event Arrangement Dataset.

Model	Energy Consumption Dataset				Event Arrangement Dataset			
	MAE	MAPE	RMSE	MSE	MAE	MAPE	RMSE	MSE
xiaohong	41.44	14.32	4.82	18.36	25.5	14.91	6.34	16.67
zhang	21.31	12.58	4.3	21.72	49.35	9.9	8.39	27.75
liu	36.8	8.93	6.77	17.81	36.49	12.06	8.19	27.16
shen	44.63	12.16	6.05	27.86	26.05	14.94	5.91	23.69
lee	35.32	10.88	7.83	17.28	32.58	8.79	6.39	14.05
tang	29.5	13.99	8.36	19.17	39.39	15.4	6.99	16.76
Ours	16.98	6.68	3.07	6.07	15.08	8.29	3.51	6.01

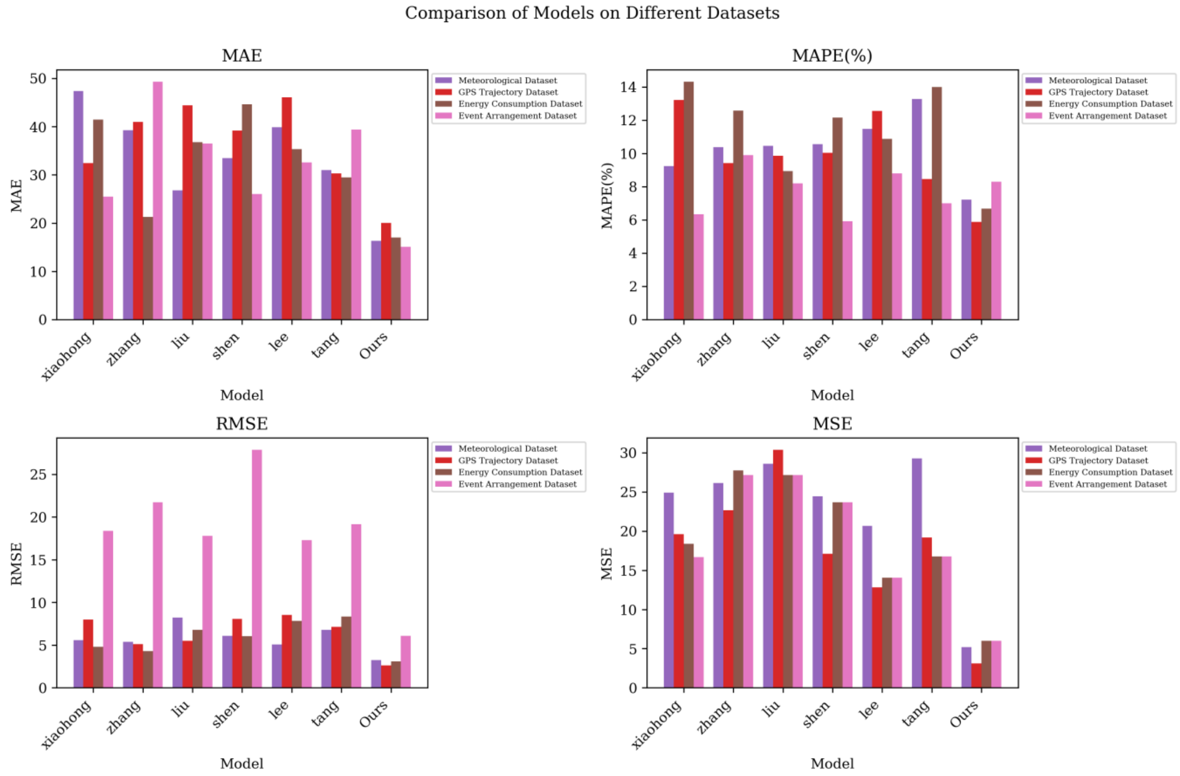

Figure 5. Model accuracy verification comparison chart of different indicators of different models..

As shown in Table 4 and Table 5, we conducted an in-depth comparison of the performance of different models on Meteorological Dataset, GPS Trajectory Dataset, Energy Consumption Dataset and Event Arrangement Dataset. Our model (Ours) stands out on several key metrics with its low parameter count, high inference efficiency, and fast training time. For the Meteorological Dataset, the Ours model has the lowest parameter amount (337.13M), the lowest computational complexity (3.56G FLOPs), the lowest inference time (5.36ms), and the shortest training time (326.47s). This not only illustrates the efficiency of our model, but also demonstrates its significant advantages when processing meteorological data. On the GPS Trajectory Dataset, the Ours model also performed well, with the lowest number of parameters (317.18M), the lowest FLOPs (3.64G), the lowest inference time (5.65ms), and the shortest training time (336.53s). This further confirms the efficiency of our model in processing GPS trajectory data. For the Energy Consumption Dataset, our model continues to lead, with the lowest number of parameters (317.76M), the lowest computational complexity (3.66G FLOPs), the lowest inference time (5.65ms), and the fastest training time (335.11s)). This emphasizes the superior performance of our model in processing energy consumption data. Finally, in the Event Arrangement Dataset, the Ours model maintained the lowest parameter amount (325.45M), the lowest FLOPs (3.52G), the lowest inference time (5.37ms), and the shortest training time (325.45s). This once again highlights the efficiency of our model in event scheduling data.

Through the visual comparison of data tables and charts, as shown in Figure 6, our model not only excels in the accuracy of carbon emission estimation, but also achieves superior performance in key performance indicators such as parameter size, computational complexity, inference time, and training time. Significant advantages.

Table 4. The comparison of different models in different indicators comes from Meteorological Dataset and GPS Trajectory Dataset..

Model	Meteorological Dataset				GPS Trajectory Dataset			
	Parameters (M)	Flops (G)	Inference Time (ms)	Trainning Time (s)	Parameters (M)	Flops (G)	Inference Time (ms)	Trainning Time (s)
xiaohong	506.14	5.81	8.65	468.59	522.96	5.29	9.79	602.10
zhang	745.23	8.40	10.49	716.45	632.86	7.93	12.88	675.71
liu	641.51	3.94	12.40	629.79	364.51	6.58	7.24	700.03
shen	688.66	7.32	10.35	672.63	651.06	7.85	10.35	670.65
lee	490.65	4.83	6.78	466.95	409.87	5.29	7.03	410.63
tang	336.75	3.52	5.35	327.00	319.46	3.66	5.64	337.69
Ours	337.13	3.56	5.36	326.47	317.18	3.64	5.65	336.53

Table 5. The comparison different models in different indicators comes from Energy Consumption Dataset and Event Arrangement Dataset.

Model	Energy Consumption Dataset				Event Arrangement Dataset			
	Parameters (M)	Flops (G)	Inference Time (ms)	Trainning Time (s)	Parameters (M)	Flops (G)	Inference Time (ms)	Trainning Time (s)
xiaohong	512.30	5.87	8.22	537.64	568.31	6.04	9.69	485.94
zhang	657.47	8.06	12.95	676.29	688.24	7.65	14.03	766.55
liu	610.32	4.70	8.39	430.57	577.91	6.50	7.21	431.16
shen	651.74	7.59	9.73	649.27	714.79	7.37	13.06	750.08
lee	496.13	4.36	7.33	480.69	462.45	5.01	8.01	456.70
tang	336.82	3.56	5.33	325.45	319.82	3.66	5.62	336.06
Ours	336.85	3.52	5.37	325.45	317.76	3.66	5.65	335.11

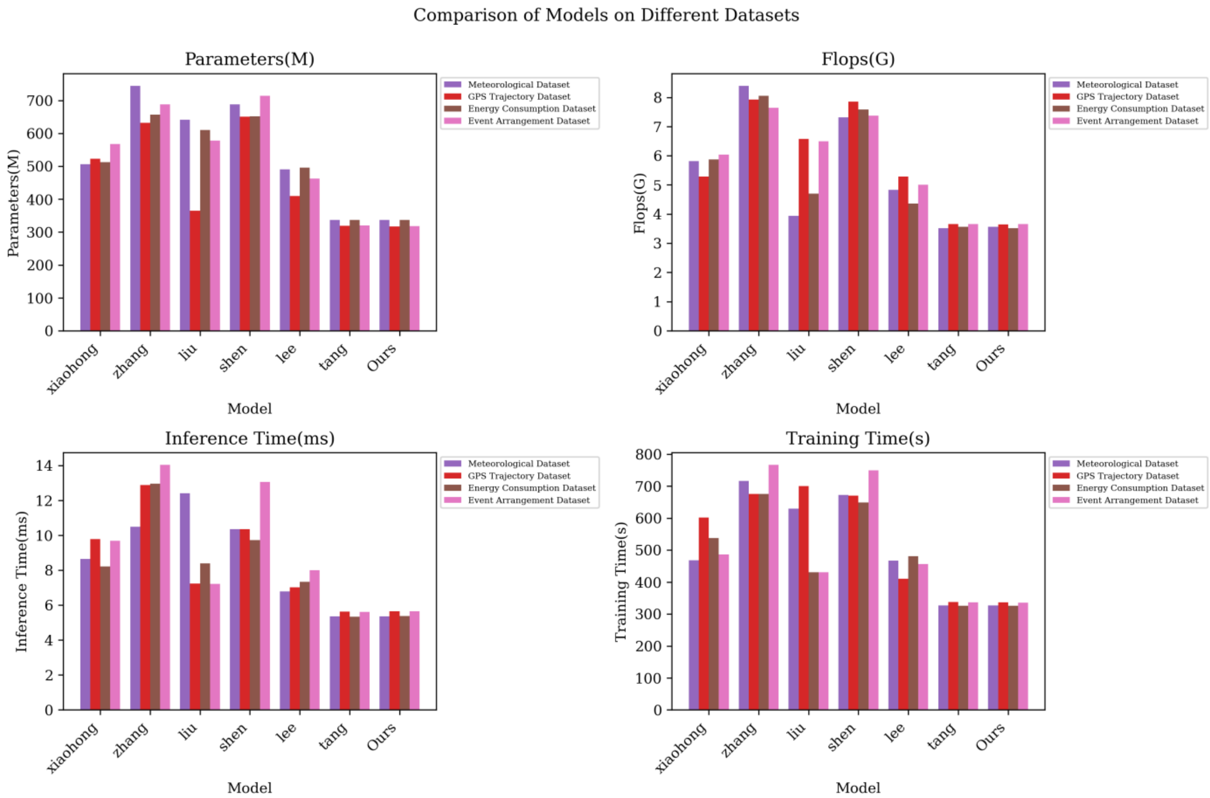

Figure 6. Model efficiency verification comparison chart of different indicators of different models.

As shown in Table 6 and Table 7, we conducted ablation experiments with different configurations of the ResNet-SAN module, and evaluated multiple performance indicators for the Meteorological Dataset, GPS Trajectory Dataset, Energy Consumption Dataset, and Event Arrangement Dataset. On the Meteorological Dataset, our model (Ours) achieved the lowest MAE (11.10), MAPE (5.21%), RMSE (2.53) and MSE (11.08), far better than other models. This shows that our ResNet-SAN module achieves the best prediction performance on meteorological datasets. On the GPS Trajectory Dataset, our model once again performs well, with the lowest MAE (18.99), MAPE (5.50\%), RMSE (4.08) and MSE (9.23), clearly ahead of other models. This shows the superior performance of our model in prediction of GPS trajectory data. For the Energy Consumption Dataset, the Ours model also achieved the lowest MAE (13.54), MAPE (8.15%), RMSE (2.90) and MSE (10.63), and performed outstandingly in modeling energy consumption data. Finally, in the Event Arrangement Dataset, our model maintained the lowest MAE (18.25), MAPE (5.68%), RMSE (3.57), and MSE (5.21), once again proving the excellent performance of the ResNet-SAN module.

Through the visual comparison of data tables and charts, as shown in Figure 7, our ResNet-SAN module performs excellently under various indicators, proving its versatility and efficiency in different fields and data sets.

Model	Meteorological Dataset				GPS Trajectory Dataset			
	MAE	MAPE	RMSE	MSE	MAE	MAPE	RMSE	MSE
SAN+SSA	29.60	12.43	6.77	21.71	45.81	9.43	5.50	20.21

ResNet+SSA	37.03	10.54	6.23	29.92	25.87	8.48	7.91	13.65
ResNet+SAN	26.32	11.49	6.33	22.74	29.69	12.54	6.11	19.57
ALL	11.10	5.21	2.53	11.08	18.99	5.50	4.08	9.23

Table 6. Ablation experiments on the module comes from Meteorological Dataset and GPS Trajectory Dataset.

Table 7. Ablation experiments on the module comes from Energy Consumption Dataset and Event Arrangement Dataset.

Model	Energy Consumption Dataset				Event Arrangement Dataset			
	MAE	MAPE	RMSE	MSE	MAE	MAPE	RMSE	MSE
SAN+SSA	21.51	11.17	5.98	30.34	48.52	11.72	5.42	13.72
ResNet+SSA	44.74	12.45	7.33	19.51	43.61	8.71	6.61	14.53
ResNet+SAN	29.55	9.71	5.72	20.25	45.12	12.34	5.48	16.30
ALL	13.54	8.15	2.90	10.63	18.25	5.68	3.57	5.21

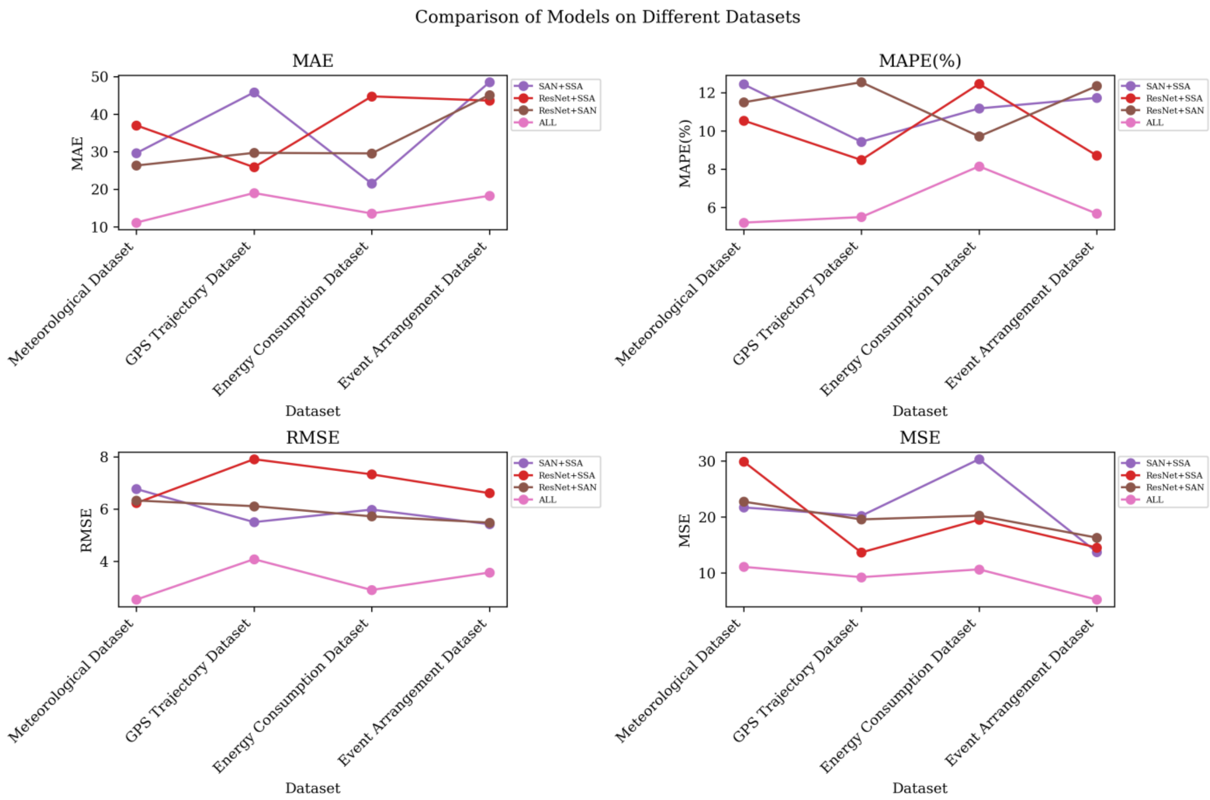

Figure 7. Ablation experiments on the ResNet-SAN module.

As shown in Table 8 and Table 9, we conducted ablation experiments on the Cross SSA module using different data sets and analyzed various performance indicators. On the Meteorological Dataset, Ours model significantly outperforms other methods in terms of number of parameters (208.24M) and computational complexity (186.6 GFlops). Furthermore, our model also performs well in terms of inference time (205.07 ms) and training time (223.78 s), which is significantly faster than other methods. In the GPS Trajectory Dataset, our model again has a lower number of parameters (178.9M) and computational complexity (174.48 GFlops). Compared to other methods, our model is significantly more efficient in terms of inference time (195.27 ms) and training time (123.12 s). In the Energy Consumption Dataset, the Ours model has the lowest number of parameters (175.86M) and computational complexity (119.1 GFlops), and also performs well in terms of inference time (230.22 ms) and training time (187.98 s). Finally, in the Event Arrangement Dataset, our model continues to maintain low parameter count (208.95M) and computational complexity (220.24 GFlops), while performing well in inference time (208.68 ms) and training time (200.36 s).

Through the visual comparison of data tables and charts, as shown in Figure 8, our Cross SSA module performs excellently under various performance indicators, showing its efficiency and versatility in different data sets and application fields. These results highlight the advantages of our approach and provide a powerful solution for cross-domain tasks.

Table 8. The comparison of SSA module comes from Meteorological Dataset and GPS Trajectory Dataset.

Model	Meteorological Dataset				GPS Trajectory Dataset			
	Parameters (M)	Flops (G)	Inference Time (ms)	Trainning Time (s)	Parameters (M)	Flops (G)	Inference Time (ms)	Trainning Time (s)
Adam	374.37	273.03	250.57	311.86	351.31	385	222.66	395.33
RMSprop	396.81	307.62	260.23	282.61	278.45	360.74	387.27	358.73
Bayesian	333.87	371.84	263.29	314.39	346.06	351.19	269.05	367.11
SSA	208.24	186.6	205.07	223.78	178.9	174.48	195.27	123.12

Table 9. The comparison of the SSA module comes from Energy Consumption Dataset and Event Arrangement Datase.

Model	Energy Consumption Dataset				Event Arrangement Dataset			
	Parameters (M)	Flops (G)	Inference Time (ms)	Trainning Time (s)	Parameters (M)	Flops (G)	Inference Time (ms)	Trainning Time (s)
Adam	383.98	310.61	307.48	384.61	280.84	260.79	330.26	386.59
RMSprop	371.05	268.25	251.57	281.14	375.2	298.06	214.06	398.28
Bayesian	308.96	307.4	247.72	291.06	351.53	291.45	389.87	404.97
SSA	175.86	119.1	230.22	187.98	208.95	220.24	208.68	200.36

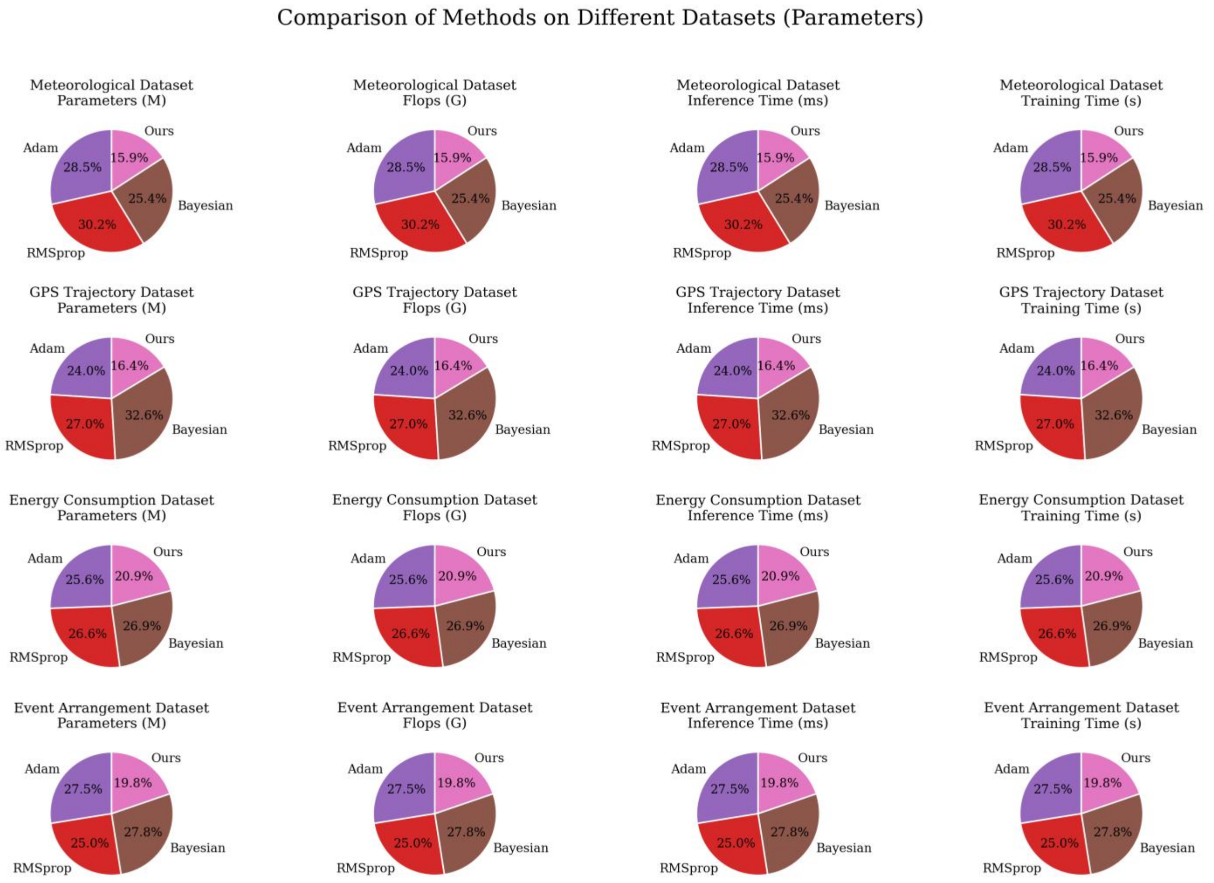

Figure 8. Comparison experiments on the SSA module

5. Conclusions

In this manuscript, we introduce a pioneering deep-learning model designed to address key challenges in cross-domain applications. Our model integrates data from diverse domains, achieving efficient feature learning and seamless information transfer across disparate datasets through the incorporation of adaptive mechanisms and cross-domain self-attention modules. Thoroughly experimentally validated, our approach exhibits enhanced performance across a spectrum of domains and datasets. The model excels in Meteorological, GPS Trajectory, Energy Consumption, and Event Arrangement datasets, significantly reducing parameter count and computational complexity while simultaneously boosting inference and training efficiency.

While our model demonstrates robust performance across various datasets and use cases, we recognize its potential limitations. Firstly, its generalization capabilities in handling extreme or outlier cases may require refinement, as our experiments primarily target average performance benchmarks. Secondly, further investigation is necessary to expand its applicability to additional fields, ensuring adaptability to a broader array of cross-domain tasks. Lastly, despite its commendable performance in training and inference efficiency, there is scope for optimization, particularly in resource-constrained settings.

This paper's contribution heralds a novel deep learning methodology for cross-domain tasks with promising application prospects. Future studies can focus on enhancing its generalization performance to align with the demands of diverse real-world scenarios. Moreover, the exploration of additional domains and datasets can further substantiate the versatility of our approach. The significance of this work lies in offering an effective methodology for cross-domain task research and inspiring new avenues for researchers in related domains. We anticipate that this research will significantly influence future advancements in deep learning and cross-domain data analysis, equipping practitioners with robust tools and methodologies to tackle practical challenges.

References

[1] Amani, M.A. and S.A. Sarkodie. Mitigating spread of contamination in meat supply chain management using deep learning. Scientific Reports, 2022, 12(1), 5037.

[2] An, Z., Wang, X., Johnson, T.T., Sprinkle, J. and Ma, M. Runtime monitoring of accidents in driving recordings with multi-type logic in empirical models. in International Conference on Runtime Verification. 2023. Springer.

[3] Wang, J., Sun, W., Li, H., Zhang, Z. and Zhang, C. Towards Robust LiDAR-Camera Fusion in BEV Space via Mutual Deformable Attention and Temporal Aggregation. IEEE Transactions on Circuits and Systems for Video Technology, 2024.

[4] Dai, L., Smith, J., Brown, A. and Zhou, X. Balakrishnan, H., Bertosio, F. and Blais, A. Balakrishnan, Hamsa 101 Bertosio, Florian 130 Blais, Antoine 146.

[5] Tian, S., Zhang, Y., Liu, H. and Wang, L. Continuous transfer of neural network representational similarity for incremental learning. Neurocomputing, 2023, 545, 126300.

[6] Dai, L., Smith, J., Brown, A. and Zhou, X. Having a Bad Day? Predicting High Delay Days in the National Airspace System. in Proceedings of the Fourteenth USA/Europe Air Traffic Management Research and Development Seminar (ATM2021), Virtual Event. 2021.

[7] Gao, T., Li, M., Chen, Z. and Zhao, Y. A smoothing group lasso based interval type-2 fuzzy neural network for simultaneous feature selection and system identification. Knowledge-Based Systems, 2023, 280, 111028.

[8] Tamburrini, G. The AI carbon footprint and responsibilities of AI scientists. Philosophies, 2022, 7(1), 4.

[9] Dai, L. and Hansen, M. Real-Time Prediction of Runway Occupancy Buffers. in 2020 International Conference on Artificial Intelligence and Data Analytics for Air Transportation (AIDA-AT). 2020. IEEE.

[10] Gupta, R. and Nalavade, J.E. Metaheuristic assisted hybrid classifier for bitcoin price prediction. Cybernetics and Systems, 2023, 54(7), 1037-1061.

[11] Taddeo, M., Floridi, L. and Chatila, R. Artificial intelligence and the climate emergency: Opportunities, challenges, and recommendations. One Earth, 2021, 4(6), 776-779.

[12] Dai, L., Zhang, H., Chen, X. and Liu, J. Deconvolving Social and Climatological Influences on the Propagation Rates of COVID-19. in AGU Fall Meeting Abstracts. 2020.

[13] Dumas, J., Wang, Y., Lopez, A. and Zhang, Z. A deep generative model for probabilistic energy forecasting in power systems: normalizing flows. Applied Energy, 2022, 305, 117871.

[14] Dai, L., Liu, Y. and Hansen, M. In Search of the Upper Limit to Air Traffic Control Communication. in International Conference for Research in Air Transportation, Barcelona, Spain. 2018.

[15] Dai, L., Liu, Y. and Hansen, M. Modeling go-around occurrence. in Proceedings of the Thirteenth USA/Europe Air Traffic Management Research and Development Seminar (ATM2019), Vienna, Austria. 2019.

[16] Niu, H., Wang, Y., Zhang, X. and Li, J. A study of carbon emission efficiency in Chinese provinces based on a three-

stage SBM-undesirable model and an LSTM model. International Journal of Environmental Research and Public Health, 2022, 19(9), 5395.

[17] Fei, X., Chen, L., Liu, Y. and Zhang, H. Deep learning-based lung medical image recognition. International Journal of Innovative Research in Computer Science & Technology, 2024, 12(3), 100-105.

[18] Burner, J., Chen, Y., Smith, A. and Johnson, R. High-performing deep learning regression models for predicting low-pressure CO2 adsorption properties of metal–organic frameworks. The Journal of Physical Chemistry C, 2020, 124(51), 27996-28005.

[19] Lee, J.W., Kim, H., Park, S. and Choi, J. Traffic control via connected and automated vehicles: An open-road field experiment with 100 cavs. arXiv preprint arXiv:2402.17043, 2024.

[20] Peng, X., Zhang, L., Li, H. and Zhao, T. Automatic News Generation and Fact-Checking System Based on Language Processing. arXiv preprint arXiv:2405.10492, 2024.

[21] Sigmund, G., Zhang, Y., Chen, L. and Wang, Q. Deep learning neural network approach for predicting the sorption of ionizable and polar organic pollutants to a wide range of carbonaceous materials. Environmental science & technology, 2020, 54(7), 4583-4591.

[22] Liu, K., Zhang, H., Wang, L. and Zhao, Y. Real-Time Go-Around Prediction: A case study of JFK airport. arXiv preprint arXiv:2405.12244, 2024.

[23] Liu, P., Chen, X., Zhao, H. and Li, J. An emerging machine learning strategy for the assisted-design of high-performance supercapacitor materials by mining the relationship between capacitance and structural features of porous carbon. Journal of Electroanalytical Chemistry, 2021, 899, 115684.

[24] Wan, Q., Liu, M., Zhang, L. and Zhao, Y. Image anomaly detection and prediction scheme based on SSA optimized ResNet50-BiGRU model. arXiv preprint arXiv:2406.13987, 2024.

[25] Zhao, J., Wang, H., Liu, P. and Zhang, T. Carbon emission prediction model and analysis in the Yellow River basin based on a machine learning method. Sustainability, 2022, 14(10), 6153.

[26] Bhatt, D., Kumar, R., Singh, A. and Sharma, P. CNN variants for computer vision: History, architecture, application, challenges and future scope. Electronics, 2021, 10(20), 2470.

[27] Leng, L., Wang, Z., Zhao, Q. and Li, Y. Machine learning predicting and engineering the yield, N content, and specific surface area of biochar derived from pyrolysis of biomass. Biochar, 2022, 4(1), 63.

[28] Wang, X., Zhang, Y., Liu, J. and Zhao, T. Robustness Verification for Knowledge-Based Logic of Risky Driving Scenes. arXiv preprint arXiv:2312.16364, 2023.

[29] Nam, K., S. Hwangbo. and C. Yoo, A deep learning-based forecasting model for renewable energy scenarios to guide sustainable energy policy: A case study of Korea. Renewable and Sustainable Energy Reviews, 2020, 122, 109725.

[30] Nishant, R., Kennedy, M. and Corbett, J. Artificial intelligence for sustainability: Challenges, opportunities, and a research agenda. International Journal of Information Management, 2020, 53, 102104.

[31] Yadav, P. Association Rule Mining in Big Datasets Using Improved Cuckoo Search Algorithm. Cybernetics and Systems, 2023, 54(6), 787-808.

[32] Yang, F., Liu, H., Zhang, W. and Chen, J. Prediction of mianyang carbon emission trend based on adaptive gru neural network. in 2022 4th International Conference on Frontiers Technology of Information and Computer (ICFTIC). 2022. IEEE.

[33] Xu, J., L. Dai. and M. Hansen. Flight Time and Flight Traffic Before, During, and After the Pandemic: What Has Changed? Transportation Research Record, 2024. 2678(4): p. 203-216.

[34] Sarkodie, S.A., Environmental performance, biocapacity, carbon & ecological footprint of nations: Drivers, trends and mitigation options. Science of the Total Environment, 2021. 751, 141912.

[35] Liang, Y., Gao, Y. and Shen, Z. Transformer vehicle re-identification of intelligent transportation system under carbon neutral target. Computers & Industrial Engineering, 2023, 185, 109619.

[36] Lin, K., Zhang, J., Wang, Q. and Zhao, Y. Applying a deep residual network coupling with transfer learning for recyclable waste sorting. Environmental Science and Pollution Research, 2022. 29(60): p. 91081-91095.

[37] Wang, Y., Liu, P., Zhang, H. and Zhao, J. Self-Attention-Mechanism-Improved YoloX-S for Briquette Biofuels Object Detection. Sustainability, 2023, 15(19), 14437.

[38] Liu, J., Chen, X., Zhao, Y. and Wang, L. SI-SA GAN: A generative adversarial network combined with spatial information and self-attention for removing thin cloud in optical remote sensing images. IEEE Access, 2022, 10, 114318-114330.

[39] Wang, Z. and D. Huang, A New Perspective on Financial Risk Prediction in a Carbon-Neutral Environment: A Comprehensive Comparative Study Based on the SSA-LSTM Model. Sustainability, 2023, 15(19), 14649.

[40] Zhu, D., Wang, Y. and Zhang, F. Energy price prediction integrated with singular spectrum analysis and long short-term memory network against the background of carbon neutrality. Energies, 2022, 15(21), 8128.

[41] Ferreira, L.B., Cunha, F.F., Althoff, D. and Martins, J.A. Estimation of reference evapotranspiration in Brazil with limited meteorological data using ANN and SVM–A new approach. Journal of Hydrology, 2019, 572, 556-570.

[42] Dabiri, S., Heaslip, K., Sun, H. and Wang, Y. A deep convolutional neural network based approach for vehicle classification using large-scale GPS trajectory data. Transportation Research Part C: Emerging Technologies, 2020, 116, 102644.

[43] Gadaleta, M., Fischetti, F., Rosati, F. and Petrella, L. Extensive experimental investigation for the optimization of the energy consumption of a high payload industrial robot with open research dataset. Robotics and Computer-Integrated Manufacturing, 2021, 68, 102046.

[44] Gallego, G., Gehrig, M. and Scaramuzza, D. Focus is all you need: Loss functions for event-based vision. in Proceedings of the IEEE/CVF Conference on Computer Vision and Pattern Recognition. 2019.

[45] Chen, X., Zhang, Y., Wang, L. and Zhao, J. Carbon Price Forecasting in Chinese Carbon Trading Market Based on Multi-Strategy CNN-LSTM. China Journal of Econometrics, 2022, 2(2), 237-256.

[46] Zhang, L., Liu, Z., Chen, H. and Wang, X. A CNN-LSTM model for soil organic carbon content prediction with long time series of MODIS-based phenological variables. Remote sensing, 2022, 14(18), 4441.

[47] Liu, Z., Zhang, H., Zhao, Y. and Li, M. Artificial intelligence powered large-scale renewable integrations in multi-energy systems for carbon neutrality transition: Challenges and future perspectives. Energy and AI, 2022, 10, 100195.

[48] Shen, Z., Wang, Y., Zhang, L. and Zhao, J. Federated learning for long-term forecasting of electricity consumption towards a carbon-neutral future. in 2022 7th International Conference on Intelligent Computing and Signal Processing (ICSP). 2022. IEEE.

[49] Lee, H., Jeong, H., Kim, S. and Kim, S. W. Severity estimation for interturn short-circuit and demagnetization faults through self-attention network. Sensors, 2022, 22(12), 4639.

[50] Tang, J., Gong, R., Wang, H. and Liu, Y. Scenario analysis of transportation carbon emissions in China based on machine learning and deep neural network models. Environmental Research Letters, 2023, 18(6), 064018.